RESEARCH ARTICLE

# Performance enhancement of OLED employing CuSCN interfacial layer

**Dinesh Chandra**[1] · **Anupam Sahu**[1] · **Brijesh Kumar**[2] ·
**Aryan Kannaujiya**[3] · **Sandeep Kumar Ojha**[1]

**Abstract** This research work outlines the effectiveness of multilayered organic light emitting diodes (OLEDs) that result in enhancement of performance of the device by incorporating a copper thiocyanate (CuSCN) interfacial layer, serving the dual purpose of facilitating hole-injection-layer and hole-transport-layer within the device. The CuSCN is used as a hole transport layer that lowered the drive voltage of OLED in the range of 1.0–1.5 V. Due to the exceptional properties of the CuSCN material, it offers distinct efficiency advantages. The upraised luminosity observed in OLEDs is attributed to a synergy between higher concentrations of electrons and holes within the emission layer. This occurrence corresponds to Langevin recombination in organic semiconductors, clarifying the process responsible for the increased luminosity. Incorporating the CuSCN layer in this investigation serves to amplify the abundant concentrations of electrons and holes in close proximity to the emission layer. The whole device behaviour is analyzed using the Silvaco Atlas tools, where, the parameters of device, including luminescent and current density are extracted. This research is precisely applicable for low-cost lighting and display applications.

## Introduction

Organic electronics is a part of electronics that deals with organics semiconductor materials [1–10]. Organics semiconductor-based diode was discovered 40 years ago but day by day it is becoming very useful and popular. When Henry by anodized aniline in sulfuric acid, obtained a partially conductive substance, which led to the discovery of electrical conduction in organic materials in 1862. Heeger, MacDiarmid, and Shirakawa investigated new material in the 1970s that after certain modifications, the polymer polyacetylene was made conductive. Tang and VanSlyke [2] realized a breakthrough by demonstrating a LED based on two organic molecules, tris (8-hydroxyquinoline) aluminium ($Alq_3$) and diamine [2].

The primary setup of OLED involves a hole injection layer (HIL), electron injection layer (EIL), and a luminescent layer. The luminescent layer, referred to as the host material or layer, comprises organic substances like $Alq_3$. The hole injection layer serves the primary function of transporting holes, while the electron injection layer (EIL) consists of an amorphous diamine film where the sole mobile carrier is electrons. OLEDs have more advantages for lighting as well as displays with the feature of light weight, flexibility, transparency, colour quality, broad

✉ Brijesh Kumar
brijeshkr@igdtuw.ac.in

Dinesh Chandra
kitestarpamu@gmail.com

Anupam Sahu
anupam.or.sahu@gmail.com

Aryan Kannaujiya
aryankannaujiya1@gmail.com

Sandeep Kumar Ojha
sandeepojhasandeep@gmail.com

1 Department of Electronics and Communication Engineering, MMMUT, Gorakhpur, India

2 Department of Information Technology, Indira Gandhi Delhi Technical University for Women, Delhi, India

3 Department of Electrical Engineering, Indian Institute of Technology , Jammu, India

size, less power consumption, and viewing angle. With the development of this modern technology of OLED, the demand of consumers is increasing, especially in the field of display devices [5].

Capitalizing on these advantages, organic electronics emerges as a preferable option for researchers investigating the subsequent technology after silicon. Consequently, researchers are actively working towards enhancing performance for optimal utilization. Various approaches are being implemented to enhance overall performance, including integrating a static aspect into material design, utilizing the vibrant properties of charge block layers in architecture, and investigating alternative materials for electrodes. Due to its large area and low power coverage; all display devices have been replaced [6–8]. Negi et al. [8] investigate how different layers in an OLED affect its performance. It is observed that the luminescence performance of the device and efficiency are being enhanced by the hole and electron block layer. According to the concept of Langevin recombination in organic semiconductors (OSC), Negi et al. [8] assessed that the substantial concentrations of electrons and holes in close proximity to the emission layer are also responsible for the heightened luminescence observed in multi-layered OLEDs.

These analyses emphasise the influence of various OLED layers, opening up new possibilities for further performance enhancement in these devices [7, 8]. The copper thiocyanate (CuSCN) thin film is introduced by Hwang et al. in 2022 as the HIL in an OLED device. The CuSCN thin film is widely recognized as an improvement in hole injection layer (HIL) and transport layer in diverse optoelectronic devices. This is due to its notable attributes, including high conductivity, a broad band gap, and cost-effective manufacturing [9–14].

The CuSCN layer lowers the cut-in voltage of the OLED [15]. Due to the low cut-in voltage of devices, there is better hole transportation in OLEDs. Due to its outstanding features like high hole mobility (ranging from 0.01 to 0.1 cm$^2$/V s), optical transparency with a wide bandgap (3.5 eV), low-temperature processing needs, and strong chemical stability, CuSCN is seen as a very promising material for hole transport applications [16–22]. The study of the multi-layered OLED's characteristic performance and its evaluation through experimentally and modeling are reported in [23–53], where various properties and performance parameters are evaluated and extracted.

In this research paper, the effectiveness of previously reported multilayer OLEDs is assessed by incorporating a layer of CuSCN inorganic material utilizing the Silvaco Technology Computer-Aided Design (TCAD) software. CuSCN material is used as a Hole Transporting material. Using this layer, the parameters of OLED such as Current density and Luminescence power have been improved.

## Architecture of the copper thiocyanate (CuSCN) based OLED device

The OLED consists of multilayer Organic semiconductor (OSC) material between two electrodes anode and a cathode. In essence, an OLED operates as a semiconductor device where the emissive layer, composed of organic materials such as QAD and Alq$_3$, emits light when an electric voltage is applied across the electrodes. In this paper, the OLED consists of a total of 9 layers among which 5 layers are organic materials and one inorganic layer CuSCN which behaves like hole transport layer between two electrodes. The five organic semiconductor layers are m-MTDATA, NPB, Alq$_3$, QAD and Alq$_3$.

In this configuration, the electron and hole charge carriers initiate movement due to the influence of the applied electric field between the anode and cathode electrodes. Electrons coming out from the cathode and holes coming out from the anode both recombine in emissive player and generate excitons. Due to the unstructured light discharge, some excitons disintegrate relative to the ground state. Therefore, the electrical energy delivered between the anode and cathode produces light. The OLEDs' lifespan is a crucial factor to take into account in addition to the device's efficiency.

In this study, we utilized the 2D atlas simulator TCAD to conduct simulations on the structure. This software provides a broad range of capabilities for simulating organic devices. Step-by-step coding can be used to explain simulation. Using the syntax of Atlas, we first define a structural mesh. A series of horizontal and vertical lines, as well as the spaces between them, can be referred to as a structure's mesh. For accurate findings and to increase the model's mathematical potency, a decent mesh is required. Following the completion of meshing, the subsequent step involves assigning the layer type to each component of the device using LiF/Al and ITO. In the last, the electrodes are specified. The structure of OLED which is simulated is shown in Fig. 1a. Table 1 show the device performance parameters used in the analysis [6, 8, 15, 44].

## Analysis of the copper thiocyanate (CuSCN) based OLED device

The following sub-sections offer a comprehensive explanation and evaluation of properties of electrical and optical of the OLED device.

### Analysis of electrical characteristics of OLED

The characteristics of electrical and optical of OLED that are connected to voltage bias situations are predicted by the ATLAS framework simulator. After defining the device, we
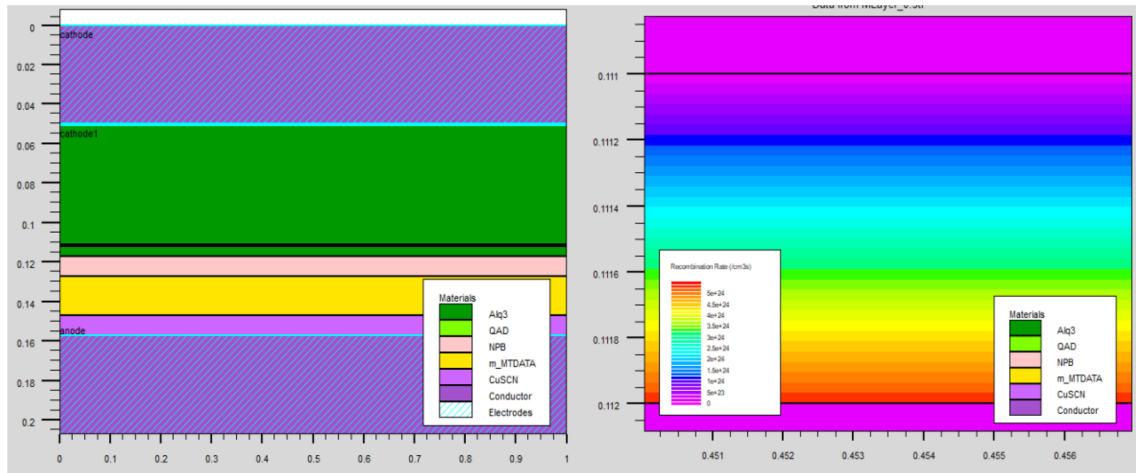
**(a)** Simulated OLED structure **(b)** Langevin Recombination in OLED.

**Fig. 1** **a** Simulated OLED structure **b** Langevin Recombination in OLED

**Table 1** Performance parameter of proposed OLED device used during simulations

| S. No | Material used in proposed OLED | Thickness (nm) |
|---|---|---|
| 1 | **Al**- Aluminium | 50 |
| 2 | **LiF**-Lithium fluoride | 10 |
| 3 | **Alq₃**-Tris(8-hydroxyquinolinato) aluminum | 60 |
| 4 | **QAD**- 5,12-dihydro-quino[2,3-b]acridine-7,14- dione or quinacridone | 10 |
| 5 | **Alq₃**-Tris(8-hydroxyquinolinato) aluminum | 50 |
| 6 | **NPB**-N,N'-DI(1-naphthyl)-N,N'-diphenyl-(1,1'-biphenyl)- 4,4'-diamine | 10 |
| 7 | **m-MTDATA**-4,4',4''-tris[phenyl(m-tolyl)amino]triphenylamine | 20 |
| 8 | **CuSCN**- Copper Thiocyanate | 10 |
| 9 | **ITO-**Indium tin oxide | 50 |

provided the polymer material parameters, such as the true refractive index, permittivity, lowest unoccupied molecular orbital (LUMO) and highest occupied molecular orbital (HOMO) levels, band gap, density of state, carrier's concentration, and lifetime, in order to forecast of characteristics of electrical and optical of the OLED. The electrical and luminescence characteristics of OLEDs are analyzed by the Poole–Fraenkel mobility and the Langevin recombination model. The various models used in OLEDs are explained here:

*Poole–Frenkel mobility model*

The luminescence characteristics and electrical parameters of OLEDs are analyzed by the Langevin recombination model and Poole–Fraenkel mobility model. At each point of mesh of the device, the variation in mobility is calculated with the help of an effective electric field. The model can be obtained from the Eq. 1 given below [8]:

$$\mu(E) = \mu_0 \exp\left[-\frac{\Delta}{KT} + \left(\frac{\beta}{KT} - \alpha\right)\sqrt{E}\right] \tag{1}$$

In Eq. 1, $\mu(E)$ denotes the mobility at electric field E. The value of $\mu(E)$ varies with the changing the value of electric field E and $\mu_0$ indicates the mobility at zero or null electric field. K denotes the Boltzmann constant (J/K) and T denotes the absolute temperature (K). Furthermore, $\Delta$ represents the activation energy under zero electric fields, while $\alpha$ serves as a fitting parameter in the analysis. Finally, the applied electric field is E and $\beta$ is the hole Poole–Frenkel factor and it is described as [8]:

$$\beta = q\sqrt{q/\pi\varepsilon\varepsilon_0} \tag{2}$$

## Langerin's recombination model

This model represents the recombination process of the charge carriers holes and electrons within the OLED. The model is expressed in Eq. 3 [8].

$$R_L(n, p) = r_1(x, y, t)\left(np - n_i^2\right) \tag{3}$$

In Eq. (3) $r_1$ denotes the recombination rate coefficient of Langevin and $n_i$ represents the concentration of intrinsic carrier. The $p$ represents the hole concentrations and $n$ represents the electrons concentrations.

Moreover, the coefficient of recombination rate of Langevin is determined using the provided expression in Eq. 4 [8].

$$r_1(x, y, t) = \frac{q\mu(E)}{\varepsilon_r \varepsilon_0} \tag{4}$$

where, q denotes the charge of carrier.$\varepsilon_r$ and $\varepsilon_0$ represents the relativity and absolute permittivity respectively. The evaluation of the device's effectiveness involves assessing luminescence power and current density under identical operating conditions, utilizing the same materials, and maintaining a consistent physical structure. Additionally, the analysis of the OLED necessitates consideration of various parameters, including the LUMO level, HOMO level, energy gap in the OSC materials, and the work function of the used electrode.

The examined characteristics of the suggested OLED, such as current density and luminescence power in relation to the applied anode voltage, are illustrated in Eqs. (3) and (4), respectively. At an input voltage of 18 V, the maximum current density reaches 743 mA/cm$^2$, while the luminescent power achieves a peak value of 0.137 cd/m$^2$.

## Internal analysis of OLED

The mathematical evaluation of the multilayer OLED is according to some common equations. These equations are employed together for the numerical assessment of the internal parameters of the OLED. The electric field within the device is computed through Poisson's equation, and the examination of charge carrier concentration and current density is performed using the drift–diffusion equation. The mobility of carriers is calculated by Poole–Frenkel model. Both models are discussed in this section. The equation of Poisson is very helpful in the measurement of the electric field inside the multilayer OLEDs. The application of voltage leads to the emergence of an electric field, which aligns with the distribution of charge carrier density within the device. The equation that describes this phenomenon is provided below [8]:

$$E\left(z + \frac{\Delta z}{2}, t\right) = E\left(z - \frac{\Delta z}{2}, t\right) + N_D(z) - N_A(z) + \nabla z \frac{q}{\varepsilon}\{p(z, t) - n(z, t)\} \tag{5}$$

In the above Eq. (5), the width of each mesh is $\Delta z$. The unit of width is in centimetres.t is the frame time for which the measurements are done. All the calculations were done in these mesh/cells of the device. E(z, t) represents the electric field at specific mesh points, while 'q' and 'ε' symbolize the charge of holes and permittivity, respectively. n (z, t) and p(z, t) denote the concentrations of electrons and holes with respect to z and t. Additionally, $N_D(z)$ and $N_A(z)$ stand for the concentrations of donor and acceptor ions at a given point z within the device. Hence, the updated dielectric field is calculated for each mesh point within the device. The units for parameters such as n(z, t), p(z, t), ND(z), and NA(z) are expressed in per cubic centimetre, indicating their densities within the device.

The migration of these charge carriers in the device occurs through the processes of drift and diffusion. Due to this migration of charge carrier the changes establish in the current as well as in electric field in the device. Equation 6 is the equation to calculate the hole density [8]:

$$p(z, t + \Delta t) = p(z, t) + r(z, t)n(z, t)p(z, t) - \Delta t \left\{ \frac{1}{q} \frac{J_p(z + (\Delta z/2), t - J_p(z - (\Delta z/2), t}{\Delta z} \right\} \tag{6}$$

However, Eq. (7) is the equation to calculate the electron density [8]:

$$n(z, t + \Delta t) = n(z, t) + r(z, t)n(z, t)p(z, t) - \Delta t \left\{ \frac{1}{q} \frac{J_n(z + (\Delta z/2), t - J_n(z - (\Delta z/2), t}{\Delta z} \right\} \tag{7}$$

where in both equations $\Delta t$ is the time step taken for calculation of charge carrier density. Further, r(z, t) is the rate of recombination of Langevin. $J_p$ indicates the hole current density and $J_n$ indicates the electron current density. Equation (8) represents the hole current density:

$$J_p\left(z + \frac{\Delta z}{2}, t\right) = q\mu_p\left(z + \frac{\Delta z}{2}, t\right)\frac{p(z, t) + p(z + \Delta z, t)}{2}E\left(z + \frac{\Delta z}{2}, t\right) - KT\mu_p\left(z + \frac{\Delta z}{2}, t\right)\frac{p(z + \Delta z, t) - p(z, t)}{\Delta z} \tag{8}$$

However, Eq. (9) represents for the electron density.

$$J_n\left(z + \frac{\Delta z}{2}, t\right) = q\mu_n\left(z + \frac{\Delta z}{2}, t\right)\frac{n(z, t) + n(z + \Delta z, t)}{2}E\left(z + \frac{\Delta z}{2}, t\right) - KT\mu_n\left(z + \frac{\Delta z}{2}, t\right)\frac{n(z + \Delta z, t) - n(z, t)}{\Delta z} \tag{9}$$

where $\mu_n$ is the mobility of electron and $\mu_p$ is the mobility of hole. The Poole–Frenkel mobility defined as:

$$\mu(E(z,t)) = \mu_0 \exp\left(\sqrt{\frac{E(z,t)}{E_0}}\right) \tag{10}$$

The characteristics of internal analysis of the proposed structure are shown in Fig. 2.

*Electric field in the device*

An electric field is the driving force for the charged carrier which flows in the electric circuit. Without the electric field, there is no any charged carrier flow in circuit. Experimental measurements and numerical device modeling are employed to investigate the internal electric field of both single and multilayer organic light-emitting diodes. This strategy produces a detailed understanding of how a multilayer OLED works.

*Singlet exciton density*

The concepts of an exciton play a role of paramount significance in the physics of organic semiconductor and interaction in organic materials. Excitons are two types: single exciton and triplet excitons. The presence of an electron–hole pair with opposing spin characterised a singlet exciton. When an electron and a hole get together due to their mutual Coulomb attraction, they create a state known as exciton. The electron releases energy after recombination in order to return to the ground state. The electron undergoes an energy loss, and this lost energy is absorbed by a photon, which then carries it away, adhering to the principle of conservation of energy. The nature of the semiconductor material significantly influences the amount of energy released in this process. In Fig. 2b shows the singlet excitons in each layer of the simulated OLED device due to the flow of current.

*Electron concentration*

Multiplying the density of states by the probability of occupancy, denoted as f(E), yields the number of electrons per unit volume within the specified energy range dE. Thus, the integral of the entire conduction energy band is the overall electron concentration. In the Fig. 2c shows the concentration of electrons in each layer of the simulated OLED device due to the flow of current. This figure shows the peaks and troughs of electrons concentration, illustrating the different layers encountered during current flow in the device.

*Hole concentration*

The quantity of holes within a given energy range, denoted as dE, can be determined by multiplying the states density by the probability of occupancy per unit volume. Thus, the integral of the entire conduction energy band is the overall hole concentration.

In Fig. 2d shows the concentration of holes in each layer of the simulated OLED device due to the flow of current. This figure shows the peaks and troughs of holes concentration, illustrating the different layers encountered during current flow in the device. Amount of energy released in this process. In the Fig. 2b shows the singlet excitons in each layer of the simulated OLED device due to the flow of current.

*Electron concentration*

Multiplying the density of available electron states by the probability of occupancy, denoted as f(E), gives the number of electrons present per unit volume within the energy interval dE. Thus, the integral of the entire conduction energy band is the overall electron concentration. In the Fig. 2c shows the concentration of electrons in each layer of the simulated OLED device due to the flow of current. This figure shows the peaks and troughs of electrons concentration, illustrating the different layers encountered during current flow in the device.

*Total current density*

The amount of total current flowing through one unit of a cross-sectional area is referred to as the current density. In Fig. 2e shows the total current density in each layer of the simulated OLED device due to the flow of current. This figure shows the peaks and troughs of total current density, illustrating the different layers encountered during current flow in the device.

## Results and discussion

This section entails the analysis and discussion of the internal behaviour of OLEDs. Following the incorporation of the CuSCN layer into the OLED structure, enhancements in parameters such as current density, luminescence power, and electron and hole recombination rates are observed and discussed. The extracted results are shown in Table 2.

### Rate of change of current density with anode voltage

Current density is the most important parameter of OLED. The examination of current density in relation to anode
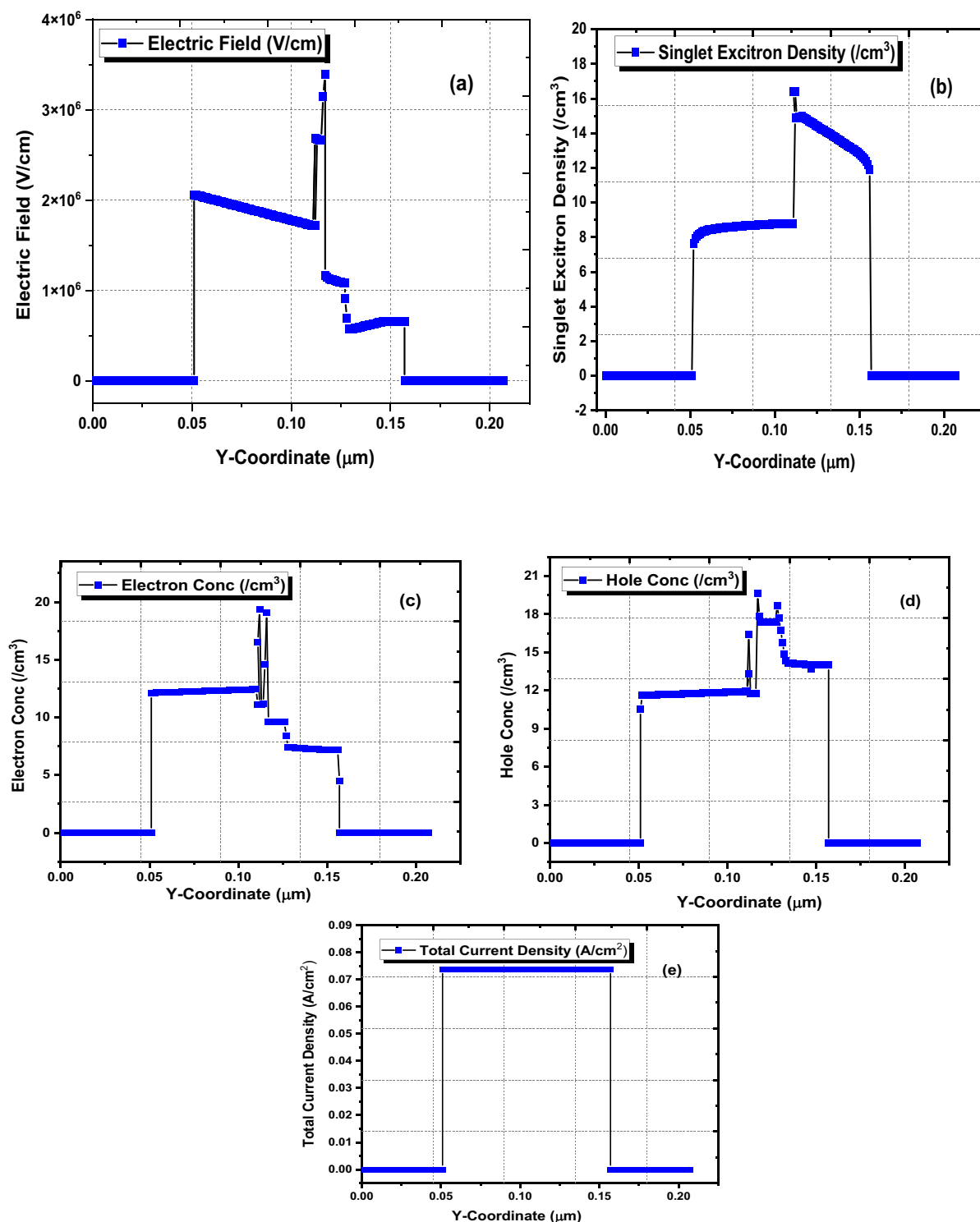
**Fig. 2** Characteristic plots **a** Electric Field, **b** Singlet exciton density, **c** Electron concentration, **d** Hole concentration, **e** Total Current density.

voltage is widely acknowledged as crucial for the proper functioning of OLEDs. Studies indicate that the rate of change of current density corresponds to the rate of carrier injection per unit area within the device structure. The anode voltage represents the forward-directed positive operational voltage applied between the anode and cathode of the OLED.

Once the electric voltage between the anode and cathode exceeds the knee voltage, the current density relative to the anode voltage starts to rise exponentially, as depicted

**Table 2** Performance outcomes of simulated multilayered OLED

| S.N | Name of parameter | Reported Device | Proposed Device |
|-----|-------------------|-----------------|-----------------|
| 1 | Current density, mA/cm$^2$ | 445.79 | 743 |
| 2 | Luminescence power, cd/m$^2$ | 0.129 | 0.137 |

in Fig. 3. In this study, the inclusion of a CuSCN layer in simulated devices leads to a decrease in the driving voltage of OLEDs. CuSCN is recognized for its function as a hole transport material, thanks to its noteworthy hole mobility falling within the range of 0.01 to 0.1 cm$^2$/V s. The use of CuSCN as a hole injection layer (HIL) has been shown to reduce the operational voltage of manufactured OLEDs by 1.0 to 1.5 V compared to the control device [45]. Due to decreased driving voltage of the OLEDs, result in enhancement of rate of change of current density. The extracted current density of the proposed device is enhanced to 743 mA/cm$^2$ at an anode voltage of 18 V.

### Rate of change of luminance power with respect to anode voltage

The effectiveness of optical devices is significantly influenced by luminance power. This segment offers a brief summary of how luminance power relates to the anode voltage in the suggested OLED. In this context, optical power refers to the brightness or intensity of light emitted from the surface of the devices. The luminescent power is influenced by factors such as the types of materials used, the number of excitons present, and the applied voltage on the OLED. Moreover, light frequency also affects the luminescent power [15].

In Fig. 3, the graph illustrates the relationship between luminescence power and applied voltage. Examining the device depicted in Fig. 1a, there is a consistent improvement in luminance power from anode voltages of 0V to 18V. Beyond 18V, the luminance power reaches a plateau, indicating a constant level. Notably, the effectiveness of the anode voltage is observed in the range of 6V to 18V for the proposed device. This suggests that the device performs optimally within this voltage range. Consequently, it can be concluded that the proposed structure exhibits superior performance with respect to the work of Negi et al. [8]. The heightened brightness illustrated in the graph shown in Fig. 2b arises from the inclusion of several electron and hole blocking layers, each having an optimal thickness, along with a thinner emissive layer. This enhancement positively impacts the luminescent output of the OLED. The extra HBL directly speeds up the electron–hole recombination rate within the emissive layer [13]. Relative to the control device,



**Fig. 3** Current density versus anode voltage for **a** Reported device **b** Proposed device and Luminescence power with respect to anode voltage **c** Reported device **d** Proposed device
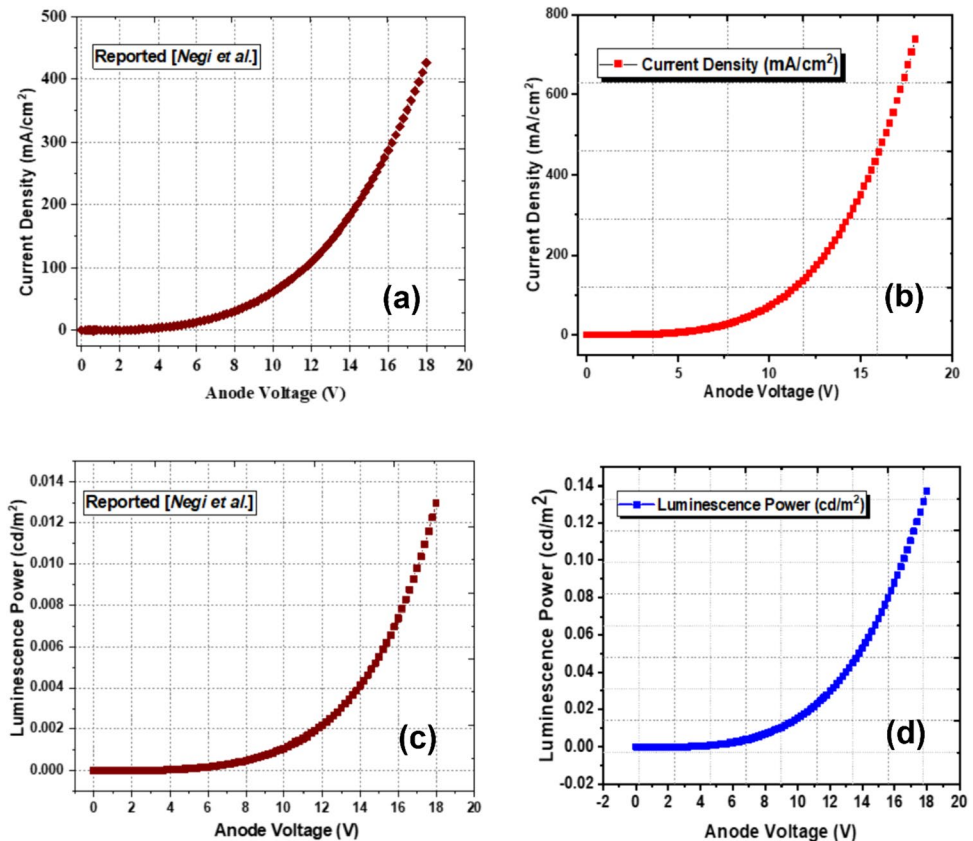
the introduction of the CuSCN layer lowers the operational voltage of the OLEDs under consideration. With a decrease in the applied voltage, the recombination of electrons and holes becomes more pronounced within the emission layer, resulting in an increase in exciton density. Consequently, with the escalating exciton density, the luminance power also experiences a corresponding increase.

## Conclusion

OLED is an organic material-based diode, widely used in display applications in mobile and television at lower cost and light weight. The commonly used electrical parameters of OLED are current density, luminescent power, and electron (hole) recombination rate etc. This research work investigated the enhancement in electrical performance of multilayered OLED device by incorporating a Copper Thiocyanate (CuSCN) interfacial layer, as the hole injection and transport layer. CuSCN material offered a distinct advantage in OLED performance that resulted in lowered the drive voltage. It has also increased luminescence of multilayered OLEDs due to augmenting the concentrations of electrons and holes near the emission layer. It was also verified by Langevin recombination principal. The entire device behaviour is analyzed using the Silvaco Atlas tools, where, the parameters of device, including luminescent and current density are extracted. This research is precisely applicable for low-cost lighting. The significant improvement in OLED performance is intended the application in display devices.

**Declarations**

## References

1. S. Negi, P. Mittal, B. Kumar, In-depth analysis of structures, materials, models, parameters, and applications of organic light-emitting diodes. J. Electron. Mater. **49**, 4610–4636 (2020)
2. C.W. Tang, S. VanSlyke, A organic electroluminescent diodes. Appl. Phys. Lett. **51**(12), 913–915 (1987)
3. C.W. Tang, S.A. Van Slyke, C.H. Chen, Electroluminescence of doped organic thin films. ppl. Phys **65**(9), 3610–3616 (1989)
4. S. Liu, R. Liu, Y. Chen, S. Ho, J.H. Kim, F. So, Nickel oxide hole injection/transport layers for efficient solution-processed organic light-emitting diodes. Chem. Mater. **26**(15), 4528–4534 (2014)
5. R.A.K. Yadav, D.K. Dubey, S.Z. Chen, T.W. Liang, J.H. Jou, Role of molecular orbital energy levels in OLED performance. Sci. Reports **101**(10), 1–15 (2020)
6. S. Negi, P. Mittal, B. Kumar, Numerical modeling and parameters extraction of novel triple hole block layer-based organic light-emitting diode for display *J. Soc. Inf Display*. **28** (12), 956–964 (2020)
7. A. Tiwari, B. Kumar, Investigation of different layer OLED structure based upon PEDOT: PSS/GO composite anode, *IEEE Int. Conf. on Electrical and Electronics Engg. (ICE3),* 14–15 February 2020, Gorakhpur, Uttar Pradesh, India 583–587 (2020)
8. S. Negi, P. Mittal, B. Kumar, Analytical modeling and parameters extraction of multilayered OLED. IET Circuits Devices Syst. **13**(8), 1255–1261 (2019)
9. J. H. Yoon, H. Chu, D. Y. Jeong, S. Choi, I. J. Hwang, S.-Y. Lee, S.-R. Kim, Decontamination of listeria monocytogens in enoki mushrooms using a 405-nm light-emitting diode illumination combined with organic acid dipping, *LWT,* 110048 (2020)
10. S. Negi, P. Mittal, B. Kumar, P.K. Juneja, Organic LED based light sensor for detection of ovarian cancer. Microelectron. Eng. **218**(15), 111154 (2019)
11. B. Kumar, C. Dubey, Performance analysis of fully flexible organic humidity sensor with top-contact and bottom-contact OTFTs. J. Semicond. Devices Circuits **6**(1), 26–34 (2019)
12. J. Akanksha, R. Mehra, design of tandem organic light emitting diode using efficient charge generation layer. Opt. Mater. **88**, 304–312 (2019)
13. E. Salsberg, H. Aziz, Degradation of PEDOT:PSS hole injection layers by electrons in organic light emitting devices. Org. Electron. **69**, 313–319 (2019)
14. S. Shahnawaz, S.S. Sudheendran, M.R. Nagar, R.A.K. Yadav, S. Gull, D.K. Dubey, J.-H. Jou, Hole transporting materials for organic light emitting diodes: An overview. J. Mater. Chem. C (2019). https://doi.org/10.1039/c9tc01712g
15. S. Negi, P. Mittal, B. Kumar, Impact of different layers on performance of OLED. Microsyst. Technol. **24**(12), 4981–4989 (2018)
16. P.J. Jesuraj, H. Hafeez, S.H. Rhee, D.H. Kim, J.C. Lee, W.H. Lee, S.Y. Ryu, Enhanced device efficiency in organic light-emitting diodes by dual oxide buffer layer. Org. Electron. **56**, 254–259 (2018)
17. J.M. Kima, J.J. Kima, Charge transport layers manage mobility and carrier density balance in light-emitting layers influencing

the operational stability of organic light emitting diodes. Org. Electron. **67**(2019), 43–49 (2018)

18. S. Negi, P. Mittal, B. Kumar, Performance analysis of double block layer OLED and variation in ratio of double block layer. Intell. Commun. Control Devices (2018). https://doi.org/10.1007/978-981-10-5903-2_14

19. S. Ohisa, T. Hikichi, Y.-J. Pu, T. Chiba, J. Kido, Two-dimensional $Ca_2Nb_3O_{10}$ perovskite nanosheets for electron injection layers in organic light-emitting devices. ACS Appl. Mater. Interfaces (2018). https://doi.org/10.1021/acsami.8b05759

20. J. Rafols-Ribe, P.A. Will, C. Hänisch, M. Gonzalez-Silveira, S. Lenk, J. Rodríguez-Viejo, S. Reineke, High-performance organic light-emitting diodes comprising ultra stable glass layers. Sci. Adv. **4**(5), eaar8332 (2018). https://doi.org/10.1126/sciadv.aar8332

21. H. Yu, H. Aziz, Exciton-induced degradation of hole transport layers and its effect on the efficiency and stability of phosphorescent organic light-emitting devices. Adv. Opt. Mater. (2018). https://doi.org/10.1002/adom.201800923

22. T. Oyamada, C. Maeda, H. Sasabe, C. Adachi, Efficient electron injection mechanism in organic light-emitting diodes using an ultra-thin layer of low-work-function metals. Japanese J. Appl. Phys. **42**(Part 2, No. 12B), L1535–L1538 (2003)

23. Y. Gao, Z. Kang, Q. Tang, G. Zhang, J. Wang, B. Bo, B. Su, Improvement of OLEDs performance with graphene doped in NPB as hole transport layer. J. Mater. Sci. Mater. Electron. **27**(6), 5676–5679 (2016)

24. Y.-F. Liu et al., Improved efficiency of indium-tin-oxide-free organic light-emitting devices using PEDOT: PSS/graphene oxide composite anode. Org. Electron. **26**, 81–85 (2015)

25. A. Kannaujiya, N. Yadava, M.D. Gupta, R.K. Chauhan, Improvement of leakage current in double pocket FDSOI 22 nm transistor using gate metal arrangement. Microw. Wirel. Technol. Lect. Notes in Electr. Eng. **877**, 2022 (2022)

26. M.T. Dang et al., Recycling indium tin oxide (ITO) anodes for use in organic light-emitting diodes (OLEDs). Thin Solid Films **638**, 236–243 (2017)

27. E. Salsberg, H. Aziz, Degradation of PEDOT: PSS hole injection layers by electrons in organic light emitting devices. *Organic Electronics,* PII-S1566119919301107 (2019)

28. Wang, Zhibin and Lu, Zhenghong. Design of high-performance organic light emitting diodes. *PhD Thesis, University of Toronto NR 97219* (2013). https://hdl.handle.net/1807/34956

29. D. Lian, K. Xie, Y. Qiu, Progress on efficient cathodes for organic light-emitting diodes. J. Soc. Inform. Display **19**(6), 453–461 (2011)

30. T. Karatsu, Materials for organic light emitting diode (OLED). *Electronic Processes in Organic Electronics Springer, Tokyo* 227–251 (2015)

31. S. Hu, J. Zeng, X. Zhu, J. Guo, S. Chen, Z. Zhao, B.Z. Tang, Universal bipolar host materials for blue, green, and red phosphorescent OLEDs with excellent efficiencies and small-efficiency roll-off. ACS Appl. Mater. Interfaces **11**(30), 27134–27144 (2019)

32. G. Shi, X. Zhang, M. Wan, S. Wang, H. Lian, R. Xu, W. Zhu, High-performance inverted organic light-emitting diodes with extremely low efficiency roll-off using solution-processed ZnS quantum dots as the electron injection layer. RSC Adv. **9**(11), 6042–6047 (2019)

33. Z. Yang, C. Cheng, X. Pan, F. Pan, F. Wang, M. Tian, H. Zhang, Effects of hole injection layer on performance of green OLEDs based on flexible ITO. Mater. Chem. Phys. **239**, 121828 (2020)

34. R. Shinar, J. Shinar, Light extraction from organic light emitting diode (OLEDs). J. Phys. Photonics (2022). https://doi.org/10.1088/25157647/ac6ea4

35. C. Murawski, M.C. Gather, Emerging biomedical applications of organic light-emitting diodes. Adv. Opt. Mater. **9**(14), 2100269 (2021)

36. J. Song, H. Lee, E.G. Jeong, K.C. Choi, S. Yoo, Organic light-emitting diodes. Push. Toward Lim. Beyond. Adv. Mater. **32**, 1907539 (2020)

37. A. Kannaujiya, A.K. Patel, S. Kannaujiya, A.P. Shah, Efficient CZTSSe thin film solar cell employing MoTe2/ MoS2 as hole transport layer. Micro Nanostructures **169**, 207356 (2022)

38. N. Satoh, T. Tanno, T. Kitabayashi, T. Kiba, M. Kawamura, Y. Abe, CaF2/ZnS multilayered films on top-emission organic light-emitting diode for improving color purity and moderation of dark-spot formation. Am. Chem. Soc. (2022). https://doi.org/10.1021/acsomega.2c01128

39. G.L. Jiménez, M.J. Rosales-Hoz, B. Handke, M.A. Leyva, C. Vázquez-López, I. Padilla-Rosales, C. Falcony, D. Dorosz, Modulating the photophysical properties of high emission Europium complexes and their processability. J. Lumin. **248**(2022), 119007 (2022). https://doi.org/10.1016/j.jlumin.2022.119007

40. R. Saha, D.A. Lyashenko, A.A. Zakhidov, Hole transport layer micro roughening for waveguide mode extraction in organic light-emitting. Diodes Phys. Status Solidi A **2022**, 2100872 (2022). https://doi.org/10.1002/pssa.202100872

41. H.U. Hwang, J. Yoon, Y.-S. Lee, J. Lee, J. Lee, K.-G. Lim, J.W. Kim, Enhanced hole injection and transport property of thermally deposited copper thiocyanate (CuSCN) for organic light-emitting diodes. APL Mater. **10**, 051109 (2022). https://doi.org/10.1063/5.0091055

42. H.-J. Kang, Y.-H. Kim, Y.H. Lee, Synthesis of protective paste for OLED panel. Adv. Sci. Technol. Lett. **98**(CES-CUBE 2015), 121–123 (2022)

43. X.A. Cao, N. Liu, D. Shelhammer, H.J. Wang, Y.M. Zhou, Stable blue fluorescent organic light-emitting diodes based on an inorganically doped homojunction. IEEE Trans. Electron Devices **68**(7), 3424–3428 (2021)

44. S. Negi, P. Mittal, B. Kumar, Modeling and analysis of high-performance triple hole block layer organic LED based light sensor for detection of ovarian cancer. IEEE Trans. Circuits Syst. I Regul. Pap. **68**(8), 3254–3264 (2021)

45. P Maurya, P Mittal, B Kumar. Performance improvement for organic light emitting diodes by changing the position of mixed-interlayer. Main Group Chemistry. **21** (3), 837-849 (2022)

46. L. Zhang, L. Wang, W.J. Wu, M. Chan, Modeling current-voltage characteristics of bilayer organic ligh-emitting diodes. IEEE Trans. Electron Devices **66**(1), 139–145 (2019)

47. L. Noroozi, H. Soofi, Controlling the electrical characteristics of charge carrier transporting layers in organic light-emitting devices by the host-guest structure: a master equation approach. IEEE Trans. Electron Devices **65**(5), 1910–1917 (2018)

48. Negi S., Mittal P., and Kumar B, Performance analysis of OLED with hole block layer and impact of multiple hole block layer. VLSI Design and Test, VDAT-2017 Communications in Computer and Information Science. **711**. 452–462 (2017)

49. B. Kumar, B.K. Kaushik, Y.S. Negi, Organic thin film transistors: structures, models, materials, fabrication, and applications: A review. Poly. Rev. **54**(1), 33–111 (2014)

50. P. Mittal, Y.S. Negi, R.K. Singh, An analytical approach for parameter extraction in linear and saturation regions of top and bottom contact organic transistors. J. Comput. Electron. **14**(3), 828–843 (2015)

51. B. Kumar, B. Kaushik, Y.S. Negi, Analysis of electrical parameters of organic thin film transistors based on thickness variation in semi-conducting and dielectric layers. IET Circuits Devices Syst. **8**(2), 131–140 (2014)

52. S. K. Paswan, D. Chandra, U. M. Bhatt, B. Kumar Performance Enhancement of CZTS and CZTSSe Solar Cells using CdS as

Buffer Layer. *International Conference on Electrical and Electronics Engineering (ICE3), 14-15 February 2020, Gorakhpur, India* (2020). https://doi.org/10.1109/ice348803.2020.9122898

53. D. Chandra, A. Sahu, A. Kannaujiya, B. Kumar, Analysis of multilayer OLED for improvement in drive current and luminescent power. *Main Group Chemistry,* **21**, 1–9, (2023)

**Publisher's Note** Springer Nature remains neutral with regard to jurisdictional claims in published maps and institutional affiliations.